

Wave and Circulation Prediction on Unstructured Grids

Joannes J. Westerink
Department of Civil Engineering and Geological Sciences
Department of Mathematics
156 Fitzpatrick Hall of Engineering
University of Notre Dame
Notre Dame, IN 46556
phone: (574) 631-6475 fax: (574) 631-9236 email: jjw@nd.edu

Clint Dawson
Department of Aerospace and Engineering Mechanics
Institute for Computational Engineering and Sciences
The University of Texas at Austin
1 University Station C0200
Austin, TX 78712
phone: (512) 475-8627 fax: (512) 471-8694 email: clint@ices.utexas.edu

Rick A. Luettich
Institute of Marine Sciences
University of North Carolina at Chapel Hill
3431 Arendell Street
Morehead City, NC 28557
phone: (252) 726-6841 ext. 137 fax: (252) 726-2426 email: rick_luettich@unc.edu

Award Number: N00014-06-1-0285
[http:// www.nd.edu/~coast](http://www.nd.edu/~coast)

LONG TERM GOALS

The long term goal of this research is to significantly advance computational models for multi-scale flow physics in geometrically and/or hydrodynamically complex oceanic and coastal ocean environments, through refinements in the defined physics, domain definition and computational grid resolution. The particular focus is on improved coupling of spectral wave models and circulation models within the framework of adaptive, parallel scalable, unstructured computational grids for ocean, coastal ocean, inlet, and inland waters.

OBJECTIVES

The objective of this project is the dynamic and tight coupling of the SWAN spectral wind wave model and the ADCIRC circulation model using identical, unstructured, large domain, computational grids. Such coupling leads to vast improvements in computational accuracy and efficiency compared to standard approaches for wave-current coupling. Implementing the wave and circulation models on unstructured grids allows for wave energy and flow processes to be optimally

Report Documentation Page				Form Approved OMB No. 0704-0188	
Public reporting burden for the collection of information is estimated to average 1 hour per response, including the time for reviewing instructions, searching existing data sources, gathering and maintaining the data needed, and completing and reviewing the collection of information. Send comments regarding this burden estimate or any other aspect of this collection of information, including suggestions for reducing this burden, to Washington Headquarters Services, Directorate for Information Operations and Reports, 1215 Jefferson Davis Highway, Suite 1204, Arlington VA 22202-4302. Respondents should be aware that notwithstanding any other provision of law, no person shall be subject to a penalty for failing to comply with a collection of information if it does not display a currently valid OMB control number.					
1. REPORT DATE 2009		2. REPORT TYPE		3. DATES COVERED 00-00-2009 to 00-00-2009	
4. TITLE AND SUBTITLE Wave and Circulation Prediction on Unstructured Grids				5a. CONTRACT NUMBER	
				5b. GRANT NUMBER	
				5c. PROGRAM ELEMENT NUMBER	
6. AUTHOR(S)				5d. PROJECT NUMBER	
				5e. TASK NUMBER	
				5f. WORK UNIT NUMBER	
7. PERFORMING ORGANIZATION NAME(S) AND ADDRESS(ES) University of Notre Dame, Department of Civil Engineering and Geological Sciences, 156 Fitzpatrick Hall of Engineering, Notre Dame, IN, 46556				8. PERFORMING ORGANIZATION REPORT NUMBER	
9. SPONSORING/MONITORING AGENCY NAME(S) AND ADDRESS(ES)				10. SPONSOR/MONITOR'S ACRONYM(S)	
				11. SPONSOR/MONITOR'S REPORT NUMBER(S)	
12. DISTRIBUTION/AVAILABILITY STATEMENT Approved for public release; distribution unlimited					
13. SUPPLEMENTARY NOTES					
14. ABSTRACT					
15. SUBJECT TERMS					
16. SECURITY CLASSIFICATION OF:			17. LIMITATION OF ABSTRACT Same as Report (SAR)	18. NUMBER OF PAGES 24	19a. NAME OF RESPONSIBLE PERSON
a. REPORT unclassified	b. ABSTRACT unclassified	c. THIS PAGE unclassified			

and locally resolved. Large domains seamlessly integrate wave and circulation physics from the deep ocean to the shelf to inlets and floodplains. The need for grid nesting and the associated problems with overlapping grids, interpolation onto nested grid boundaries, and two way communications between nested grids are all eliminated. The application of identical unstructured grids leads to improvements in accuracy since the need to interpolate between heterogeneous grids is eliminated, avoiding the associated aliasing of inter-code solutions and forcing functions. In addition, resolution requirements in the wave and circulation models are often similar due to the response-forcing function interaction of the two models. Finally the use of identical unstructured grids provides enormous efficiencies in parallel computing, since inter-code communications is intra-core.

We also want to continuously improve scalability in order to be able to simulate larger and better resolved grids on the ever evolving parallel computer systems. Furthermore we want to automate the definition of the unstructured grids for the next generation of wave-circulation models within the framework of *hp*-adaptive discontinuous Galerkin (DG) based solutions. These methods optimize the application of high resolution zones to correctly capture the wave-circulation coupling within high gradient surface water elevation, current, and wave transformation zones without over-resolving adjacent areas, effectively optimizing the accuracy of a given computation for a specified cost.

APPROACH

We have focused on three areas to accomplish the defined objectives. The first area is integrating the SWAN wave and ADCIRC circulation model in such a way as to maximize the accuracy and scalability of the combined models. The goal is to remain scalable and efficient up to 10,000's of processors and to achieve wall clock times that allow for forecasting. The SWAN and ADCIRC model components are applied to the identical, unstructured grid; share parallel computing infrastructure; and run sequentially in time. Wind speeds, water levels, currents and radiation stress gradients are node-based, and therefore can be passed through memory or cache to each model component. Parallel simulations based on domain decomposition utilize identical sub-grids, and the communication is highly localized. Inter-model communication is intra-core, while intra-model communication is inter-core but is local and efficient because it is solely on adjacent sub-grid edges. This communications paradigm is summarized in Figure 1. The resulting integrated SWAN+ADCIRC system is highly scalable and allows for localized increases in resolution without the complexity or cost of nested grids or global interpolation between heterogeneous grids. Extensive verification against analytical solutions has been performed to demonstrate consistency and evaluate convergence. Hurricane waves and storm surge have been validated for Hurricanes Katrina (2005), Rita (2005) and Ike (2008). Efficiency for operational models is demonstrated for large grids which require less than 20 minutes of wall clock time per day simulation.

The second area is evaluating performance and scalability enhancements for Continuous Galerkin (CG) and Discontinuous Galerkin (DG) implementations of ADCIRC. Detailed analyses of the current operational CG version of ADCIRC indicate that scalability of the implicit code is limited by the global communications necessary for the matrix solution. Analysis indicates that explicit CG implementations are not only faster but have even better scalability. Furthermore investigations of the scalability of DG based solutions show that they are also better than the CG based implicit solutions along with improvements in accuracy on a per degree of freedom basis.

The third focus area is developing *hp*-adaptive schemes for DG solutions to the shallow water equations (SWE) in anticipation of coupling with a DG based grid adaptive versions of the SWAN wave model. This will improve the unstructured grid capabilities for the ADCIRC circulation model by dynamically improving resolution and ensuring that sufficient grid resolution is provided for all relevant flow scales. DG algorithms are particularly well-suited for both propagation and advection dominated problems with or without sharp gradients in the forcing function, bathymetry, and/or flow. DG methods inherently preserve mass perfectly on an elemental level, which make them ideal for coupling flow and transport models. Example problems include flows with strong eddies such as those issuing from and through inlets; flows through rapidly varying bathymetry such as canyons or deep scour holes in inlets; and flows with sharp fronts such as tidal bores, ebb tide – waves interactions in inlets and wetting fronts. DG methods are conceptually similar to finite volume methods although DG methods are readily implemented with higher-order bases. DG methods are also ideal since non-conforming h and p refinement and adaptivity can be implemented. In addition, DG methods are significantly more accurate on a per degree of freedom basis than CG methods.

WORK COMPLETED

The SWAN+ADCIRC code has been completed and the resulting tightly coupled scalable parallel unstructured grid wave-current model has been thoroughly validated (Dietrich et al. 2009b). The parallel implementation of unstructured SWAN uses ADCIRC's highly efficient and scalable parallel MPI based communications subroutines. This synergy allowed for the very rapid development of the parallel unstructured grid version of SWAN by Delft University. The SWAN+ADCIRC code has been verified and validated and is already being used by numerous researchers around the world. The resulting SWAN+ADCIRC model will be released as a Gnu licensed combined code for use as a community model.

The efficiency of the CG solutions to the SWE's has been a matter of intensive study. The scalability and efficiency of CG based SWE solutions can be dramatically improved through explicit implementations (Tanaka et al., 2009). The improvements come from the elimination of the MPI All Reduce calls used in the Conjugate Gradient matrix solver which requires all computational cores to communicate with each other. It is noted that explicit time stepping is not a limitation on time step which is in fact controlled by wetting front propagation speeds and accuracy concerns. We have also completed a comparison study of DG and CG methods that finds that for comparable accuracy, both methods have very similar computational costs (Kubatko et al., 2009a).

Detailed studies of the time step limitation of the two-dimensional RKDG SWE solutions were performed to examine the stability properties of these solutions (Kubatko et al., 2008). Semi discrete DG approximations using polynomials spaces of degree $p = 0, 1, 2$, and 3 were considered and discretized in time using a number of different strong-stability-preserving (SSP) Runge–Kutta time discretization methods. Approximate relations between the two dimensional CFL conditions were derived and numerical results verify the CFL conditions that were obtained, and “optimal”, in terms of computational efficiency.

Improvements have been made for DG based implementations in the robustness and accuracy of the RKDG SWE based wetting/drying algorithm, including proving convergence for a range of problems (Bunya et al., 2009a). The new wetting and drying treatment was verified through comparisons with five problems with exact solutions and convergence rates were examined.

The DG SWE code p - (polynomial order) and standard h - (grid) refinement/adaptivity options have been further refined and our progress is summarized by Kubatko et al. (2009b). Further improvements in DG efficiency are being made by implementing quadrilaterals. In addition to having advantages from a degree of freedom perspective for low order interpolation, quadrilaterals have distinct advantages from the perspective of improvements in accuracy for a specific cost (Wirasaet et al., 2009).

Validation of the DG SWE code has been performed by studying tides in the western North Atlantic (Kubatko et al., 2009b) as well as in Pacific Ocean inlets. We have also applied DG based algorithms to hurricane problems in Texas. The DG solutions are stable, robust and perform well.

RESULTS

The details of the SWAN+ADCIRC model implementation are described by Dietrich et al., 2009b. We have verified that the physics of wave induced coastal setup is correctly modeled. Here we briefly describe the validation of the coupled model in computing hurricane waves in the Gulf of Mexico for Hurricanes Katrina and Ike. SWAN+ADCIRC utilize the SL15 grid, Figure 2 and 3, which has been validated for applications in southern Louisiana (Bunya *et al.*, 2009b; Dietrich *et al.*, 2009a). This grid incorporates local resolution down to 50m, and extends to the Gulf of Mexico and the western North Atlantic Ocean, Figure 4. It includes a continental shelf that narrows near the protruding delta of the Mississippi River, sufficient resolution of the wave-transformation zones near the delta and over the barrier islands, and intricate representation of the various natural and man-made geographic features that collect and focus storm surge in this region. The SL15 grid contains 2,409,635 nodes and 4,721,496 triangular elements. Details of all parameter selections for both SWAN and ADCIRC are given by Dietrich et al. (2009b).

Figure 5 depicts the computed significant wave heights at 12-hr intervals as Katrina enters the Gulf, generates waves throughout the majority of the basin, and then makes landfall in southern Louisiana. In its early stages, Katrina generated significant wave heights of 6-9m in the eastern half of the Gulf. However, as the storm strengthened on 28 August 2005, the significant wave heights increased to a peak of about 22m at 2200 UTC, and waves of at least 3m were generated throughout most of the Gulf. SWAN+ADCIRC has been validated to a variety of wave and water level measurement data sets. In deep water, the National Data Buoy Center (NDBC) collected and analyzed wave measurements at 12 buoys. Figure 6-8 compare measured significant heights, mean directions and mean periods to computed values from SWAN+ADCIRC as well as with results from the WAM model. SWAN matches the measurements well at most buoys, and in fact the results are quite similar to WAM. Extensive comparisons to all data are presented by Dietrich et al. (2009b)

Figure 9 shows the evolution of Hurricane Ike while it tracked through the Gulf of Mexico with significant heights reaching about 19m, and large waves being generated throughout the entire Gulf. The SWAN wave solution for Ike has been compared to measured results from NDBC buoys. The significant wave heights, directions and mean periods, shown in Figure 10 through 12 suggest that SWAN+ADCIRC is performing as well for Ike as it did for Katrina and Rita.

SWAN+ADCIRC was benchmarked on Ranger, a Sun Constellation Linux Cluster with 62,976 cores, at the Texas Advanced Computing Center (TACC) (<http://www.tacc.utexas.edu>). Simulations

were performed with the coupled model and again with its individual components in order to discern coupling effects on simulation times. The models were run on 256 to 5,120 cores. As shown in Figure 13, the individual SWAN and ADCIRC models both scale linearly through about 1,000-1,500 cores, but they diverge at higher numbers of computational cores. ADCIRC's timing results level off, because the global communication associated with its implicit, conjugate-gradient solver begins to dominate the simulation time. The highly localized solution procedure in SWAN allows it to scale linearly through 5,000 cores, enabling performance of less than 5 min per day of Katrina simulation. Also note the coupled model shows linear scaling to about 3,000 computational cores, but then it levels off. At this point, the communication overhead from ADCIRC implicit CG solution slows down the coupled model. However, the performance in this range is about 20 min per day of Katrina simulation, which is sufficient for forecasts of large storms.

Tanaka et al. (2009) investigated the scalability of implicit and explicit versions of the CG implementation of ADCIRC. Figure 14 compares explicit and implicit simulations of the SL15 grid (2,351,832 nodes) and a uniformly refined by a factor of four version of the grid, SL15-04x (9,314,706 nodes). We note that the explicit simulations are about twice as fast as the implicit implementations. More importantly, the implicit code shows weak parallel scaling with a limit in scalability that is improved with larger grids. However, the explicit code shows much improved scalability compared to the implicit code. Figure 15 and 16 show that this is largely related to the MPI All Reduce in the required global communications in the matrix solver in the implicit code. This then suggests that the CG implementation of ADCIRC be run explicitly, resulting in further improvements in scalability of the SWAN+ADCIRC code. A study of the performance of the DG implementation of ADCIRC was also done showing that the explicit DG code performs much better in terms of scaling than the CG code (Kubatko et al., 2009a).

The development of the DG based implementation in terms of explicit time stepping, wetting-drying, and *h-p* adaptivity and are summarized by Kubatko et al. (2008), Bunya et al. (2009a), and Kubatko et al. (2009b). Wirasaet et al. (2009) describe the development and use of quadrilaterals within the DG framework in order to gain further efficiencies in accuracy versus cost.

Detailed studies of tidal elevations and currents in Willapa Bay, WA show that the DG based solutions perform well in areas characterized by its large tidal range, fast currents, strong advection, and large tidal flats. We have also applied DG based solutions to compute storm surge during Hurricane Ike along the Texas coastline, Figure 17 and 18. The computations are stable and robust.

IMPACT/APPLICATIONS

This work will significantly improve the accuracy of the computed physics for coupled coastal ocean wave and circulation computations. The physics will be directly improved through the much tighter wave – circulation model coupling, as well as through the ability to apply much higher resolution grids which will in fact refine themselves to the appropriate levels through the DG adaptivity. This work will also reduce model development times since the base grids developed by hand only need to represent the geometry and not the hydrodynamics. The grids will adjust themselves automatically and optimally to account for the waves and currents as the hydrodynamics evolves in the simulation.

PUBLICATIONS

Bunya, S., E.J. Kubatko, J.J. Westerink, C. Dawson, “[A Wetting and Drying Treatment for the Runge-Kutta Discontinuous Galerkin Solution to the Shallow Water Equations](#),” *Computer Methods in Applied Mechanics and Engineering*, **198**, 1548-1562, 2009a.

Bunya, S., J.C. Dietrich, J.J. Westerink, B.A. Ebersole, J.M. Smith, J.H. Atkinson, R. Jensen, D.T. Resio, R.A. Luetlich, C. Dawson, V.J. Cardone, A.T. Cox, M.D. Powell, H.J. Westerink, H.J. Roberts, “[A High Resolution Coupled Riverine Flow, Tide, Wind, Wind Wave and Storm Surge Model for Southern Louisiana and Mississippi: Part I - Model Development and Validation](#),” *Monthly Weather Review*, In Press, DOI: 10.1175/2009MWR2907.1, <http://ams.allenpress.com/perlserv/?request=get-abstract&doi=10.1175%2F2009MWR2907.1>, 2009b.

Dietrich, J.C., S. Bunya, J.J. Westerink, B.A. Ebersole, J.M. Smith, J.H. Atkinson, R. Jensen, D.T. Resio, R.A. Luetlich, C. Dawson, V.J. Cardone, A.T. Cox, M.D. Powell, H.J. Westerink, H.J. Roberts, “[A High Resolution Coupled Riverine Flow, Tide, Wind, Wind Wave and Storm Surge Model for Southern Louisiana and Mississippi: Part II - Synoptic Description and Analyses of Hurricanes Katrina and Rita](#),” *Monthly Weather Review*, In Press, DOI: 10.1175/2009MWR2906.1, <http://ams.allenpress.com/perlserv/?request=get-abstract&doi=10.1175%2F2009MWR2906.1>, 2009a.

Dietrich, J.C., M. Zijlema, J.J. Westerink, L.H. Holthuijsen, C. Dawson, R.A. Luetlich, R. Jensen, J.M. Smith, G.S. Stelling, G.W. Stone, “Modeling Hurricane Waves and Storm Surge using Integrally-Coupled, Scalable Computations,” *Journal of Oceanic and Atmospheric Technology*, To be submitted, 2009b.

Kubatko, E.J., C. Dawson, J.J. Westerink, “[Time Step Restrictions for Runge-Kutta Discontinuous Galerkin Methods on Triangular Grids](#),” *Journal of Computational Physics*, **227**, 9697-9710, 2008.

Kubatko, E.J., S. Bunya, C. Dawson, J.J. Westerink, C. Mirabito, “[A Performance Comparison of Continuous and Discontinuous Finite Element Shallow Water Models](#),” *Journal of Scientific Computing*, **40**, 315-339, 2009a.

Kubatko, E.J., S. Bunya, C. Dawson, J.J. Westerink, “[Dynamic \$p\$ -adaptive Runge-Kutta Discontinuous Galerkin Methods for the Shallow Water Equations](#),” *Computer Methods in Applied Mechanics and Engineering*, **198**, 1766-1774, 2009b.

Tanaka, S., J.J. Westerink, C. Dawson, R.A. Luetlich, “Scalability of an Unstructured Grid Continuous Galerkin Based Hurricane Storm Surge Model,” *Journal of Scientific Computing*, In Preparation, 2009.

Wirasaet, D., S. Tanaka, E.J. Kubatko, J.J. Westerink, C. Dawson, “A Performance Comparison of Nodal Discontinuous Galerkin Methods on Triangles and Rectangles,” *International Journal for Numerical Methods in Fluids*, To be submitted, 2009.

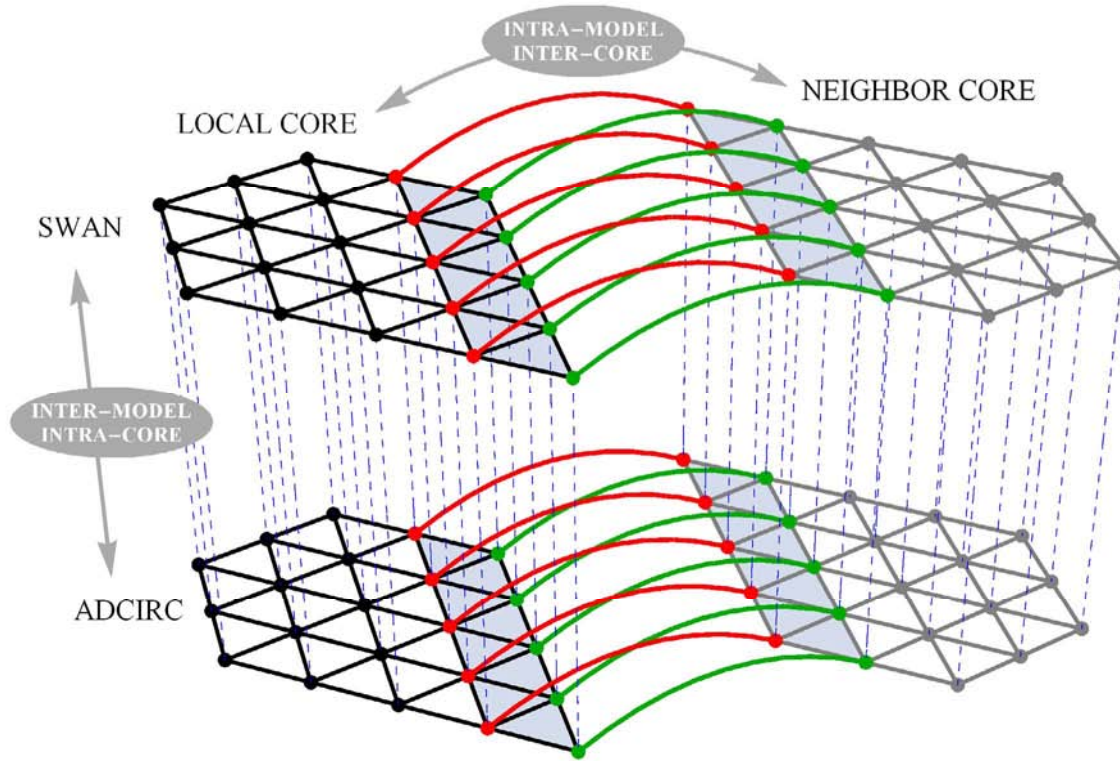


Figure 1. Schematic of parallel communication between models and cores. Dashed lines indicate communication for all nodes within a sub-grid, and are inter-model and intra-core. Solid lines indicates communication for the edge-layer-based nodes between sub-grids, and are intra-model and inter-core.

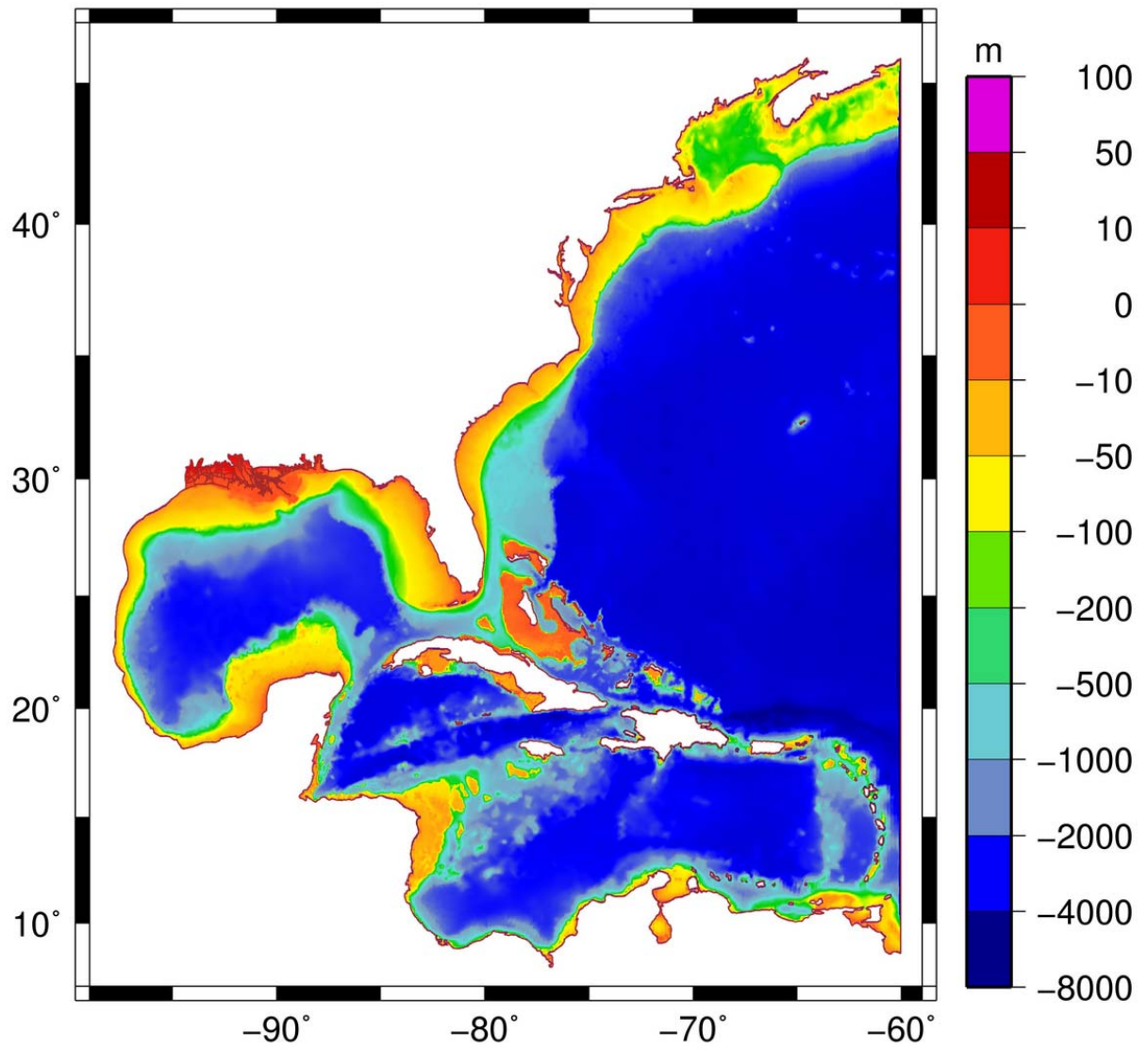


Figure 2: ADCIRC SL15 model domain with bathymetry (m).

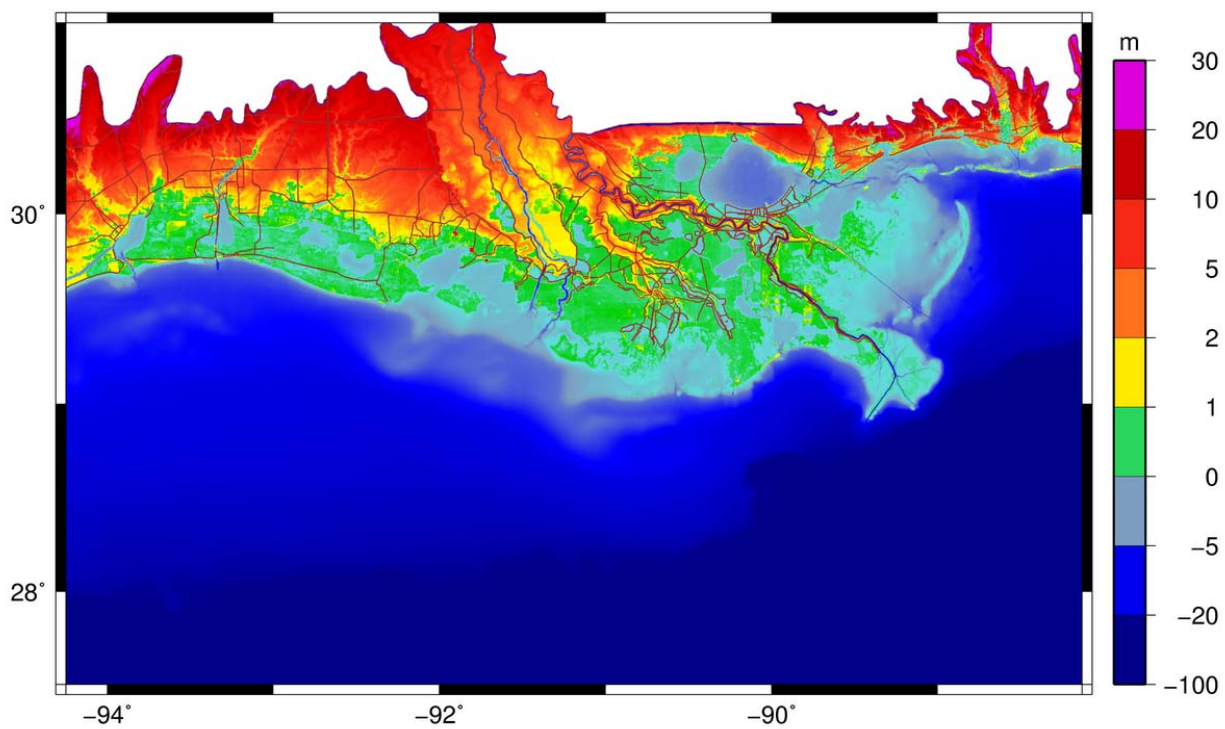


Figure 3: ADCIRC SL15 bathymetry and topography (m), relative to NAVD88 (2004.65), for southern Louisiana.

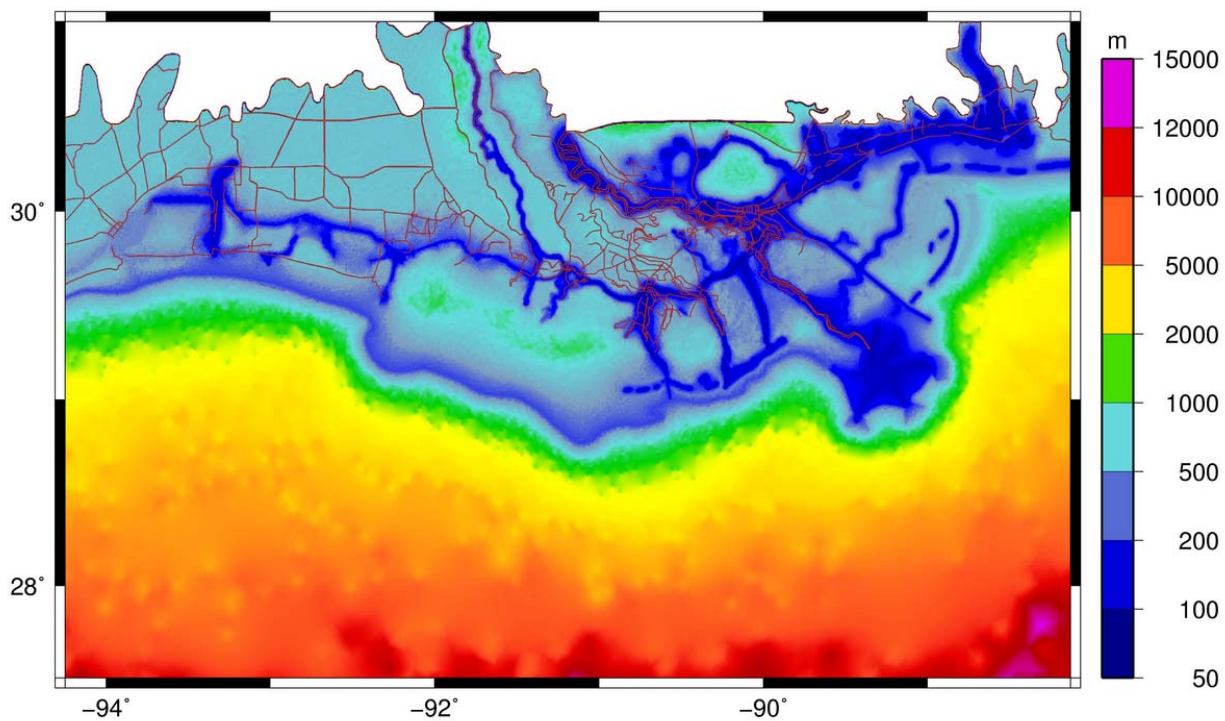


Figure 4: ADCIRC SL15 grid resolution (m) in southern Louisiana.

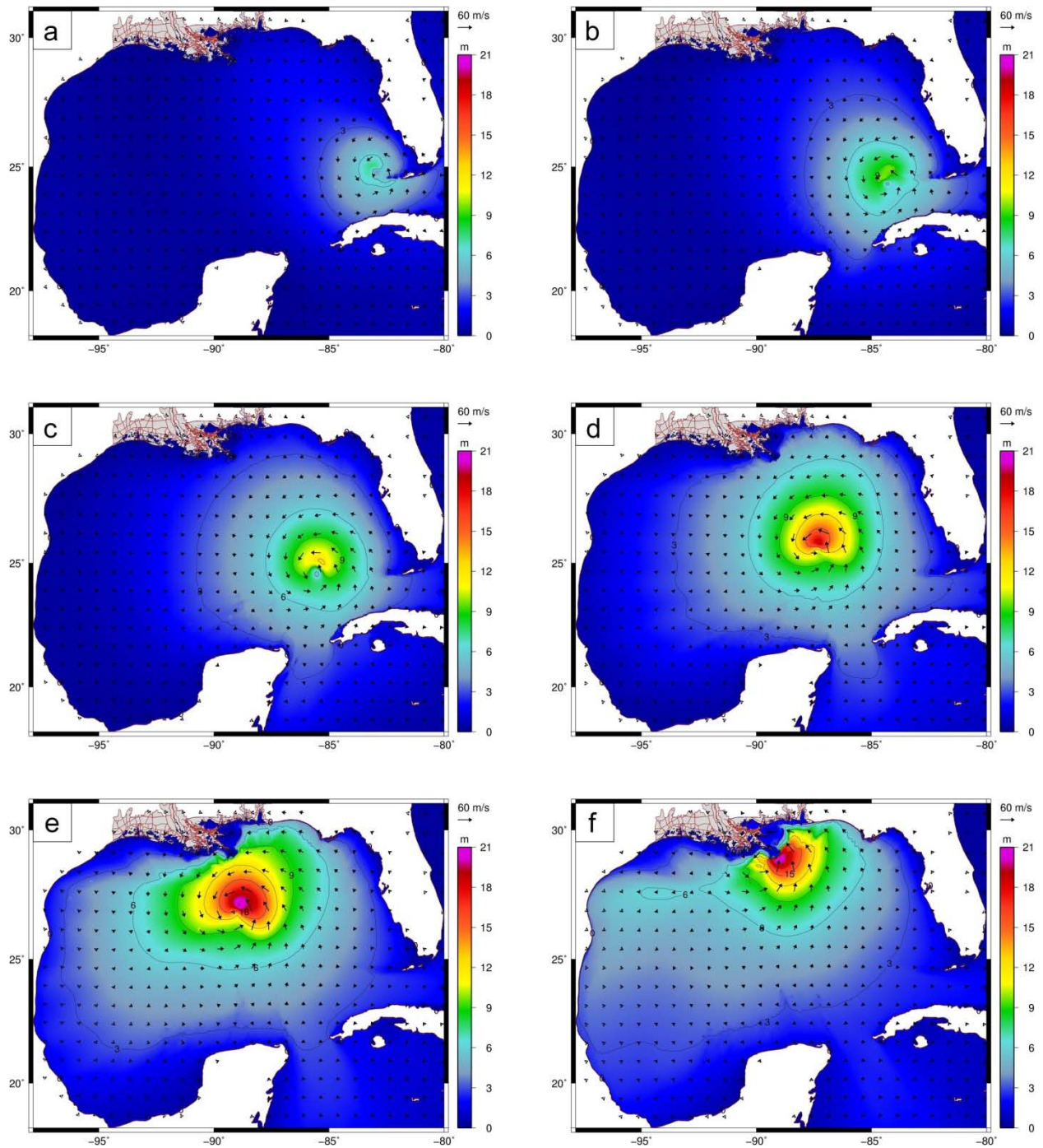


Figure 5: Hurricane Katrina significant wave height contours (m) and wind speed vectors ($m s^{-1}$) at 12-hr intervals in the Gulf of Mexico. The six panels correspond to the following times: (a) 2200 UTC 26 August 2005, (b) 1000 UTC 27 August 2005, (c) 2200 UTC 27 August 2005, (d) 1000 UTC 28 August 2005, (e) 2200 UTC 28 August 2005 and (f) 1000 UTC 29 August 2005.

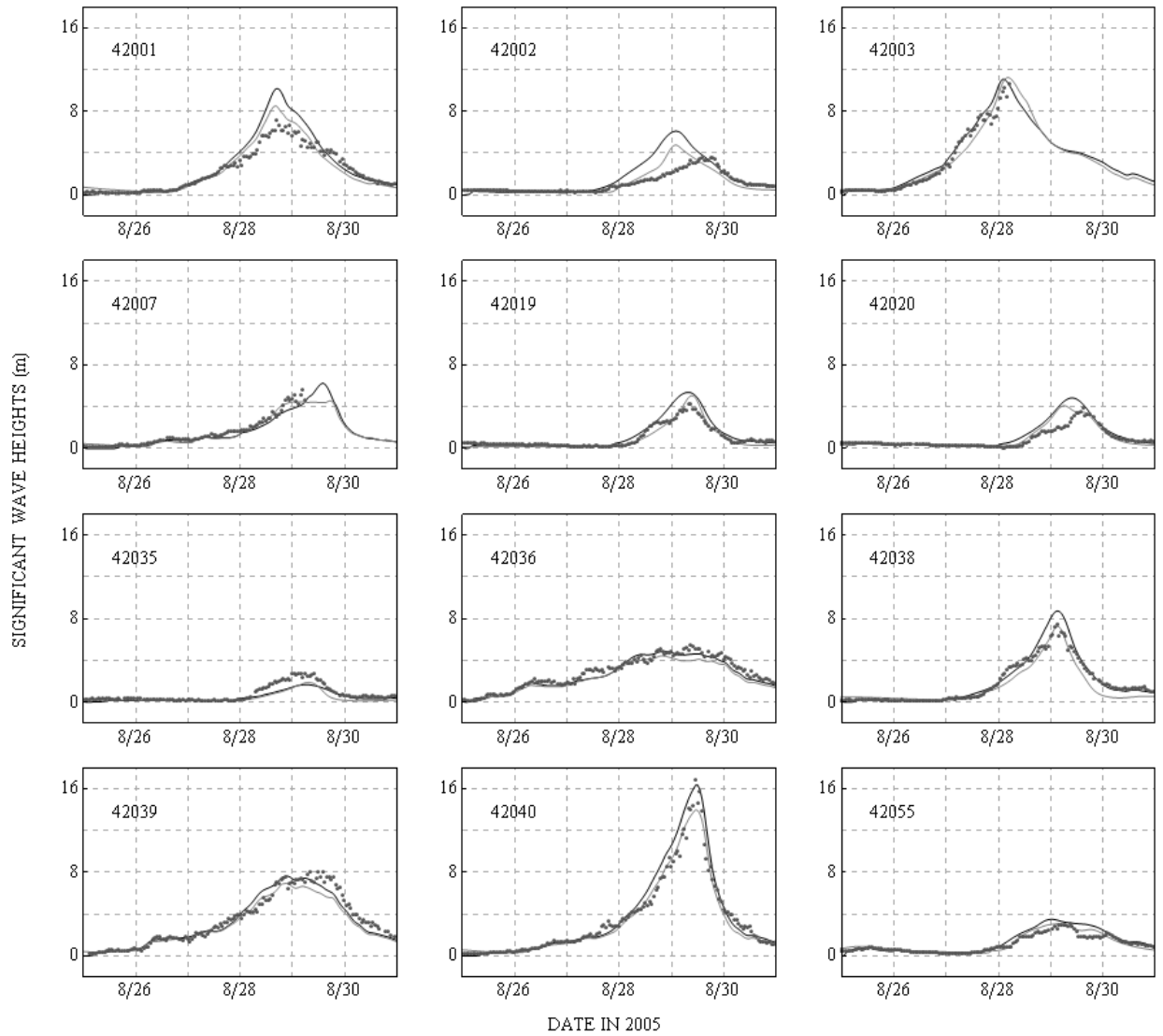


Figure 6: Significant wave heights (m) during Hurricane Katrina at 12 NDBC buoys. The measured data is shown with black dots, the modeled SWAN results are shown with black lines, and the modeled WAM results are shown with gray lines.

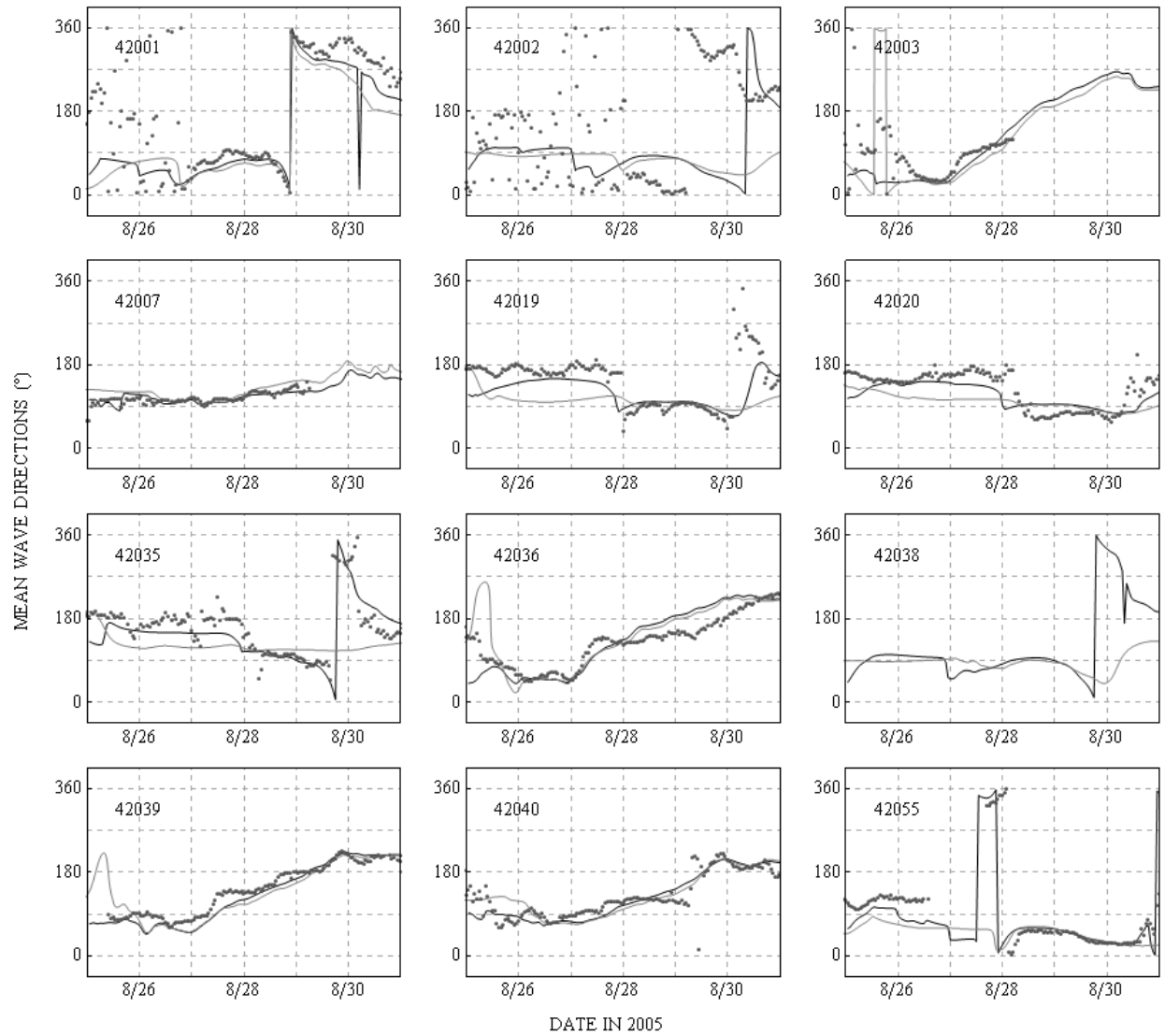


Figure 7: Mean wave directions (°), measured clockwise from geographic north, during Hurricane Katrina at 12 NDBC buoys. The measured data is shown with black dots, the modeled SWAN results are shown with black lines, and the modeled WAM results are shown with gray lines.

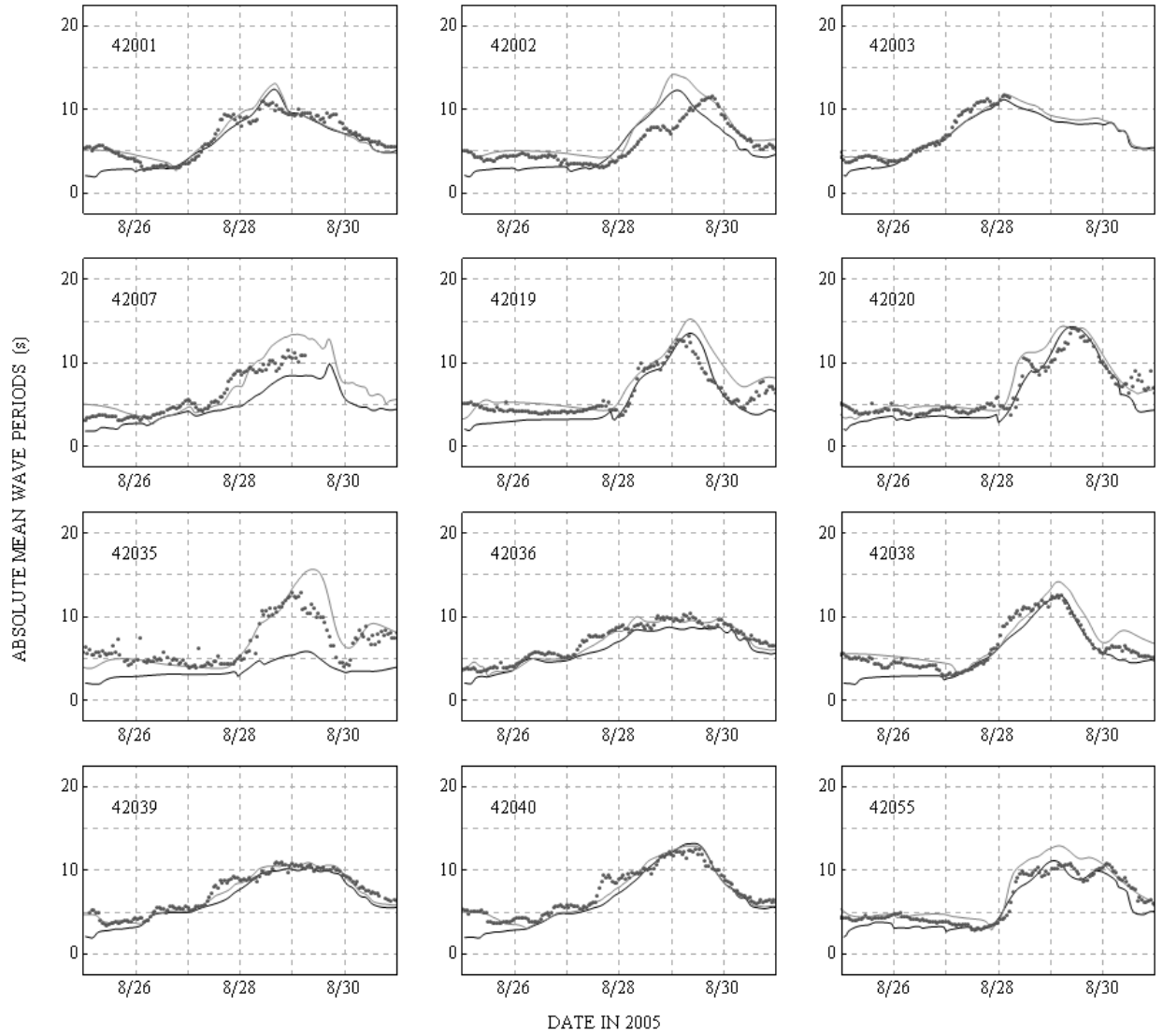


Figure 8: Mean wave periods (s) during Hurricane Katrina at 12 NDBC buoys. The measured data is shown with black dots, the modeled SWAN results are shown with black lines, and the modeled WAM results are shown with gray lines.

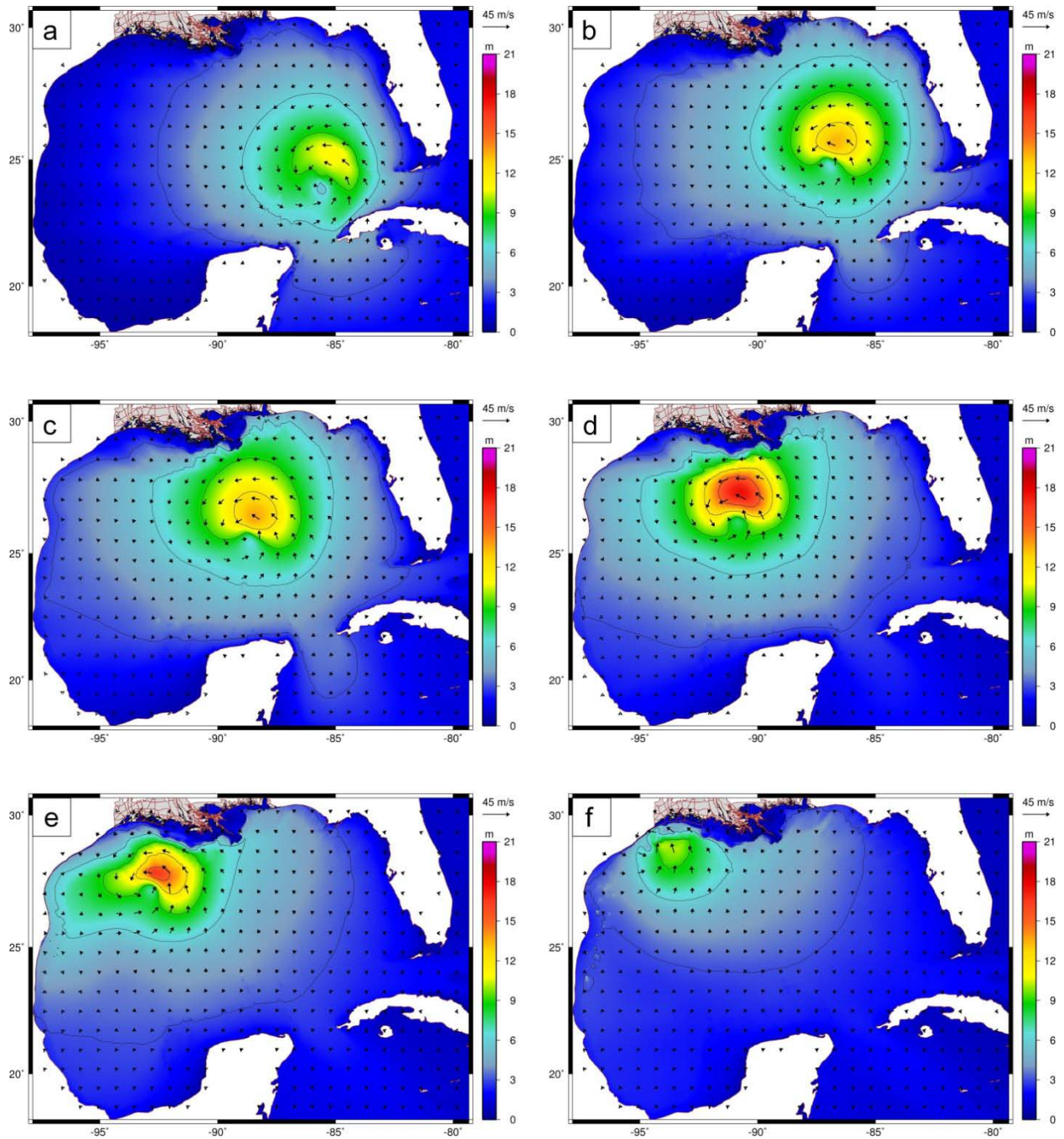


Figure 9: Hurricane Ike significant wave height contours (m) and wind speed vectors (m s^{-1}) at 12-hr intervals in the Gulf of Mexico. The six panels correspond to the following times: (a) 1800 UTC 10 September 2008, (b) 0600 UTC 11 September 2008, (c) 1800 UTC 11 September 2008, (d) 0600 UTC 12 September 2008, (e) 1800 UTC 12 September 2008 and (f) 0600 UTC 13 September 2008.

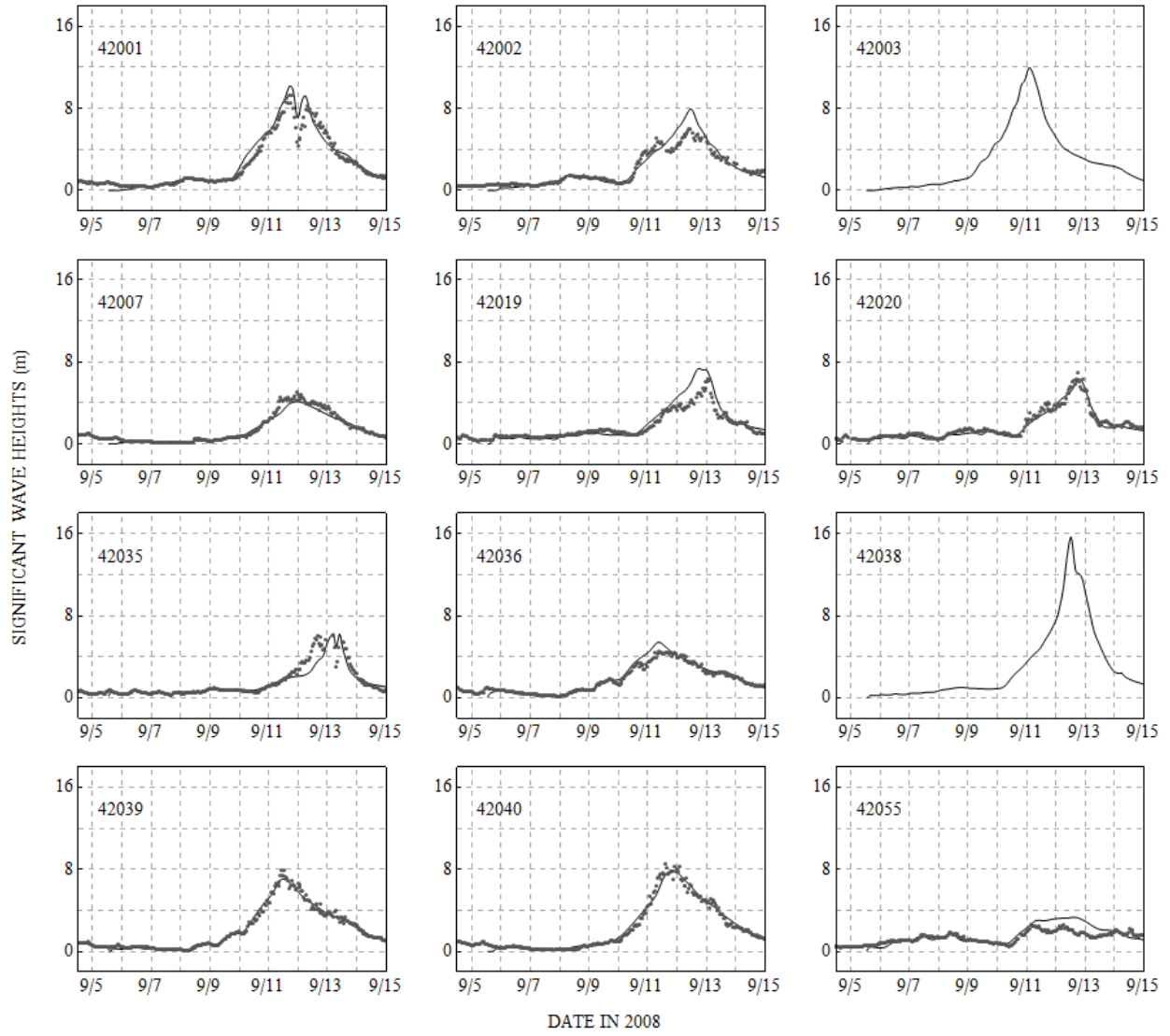


Figure 10: Significant wave heights (m) during Hurricane Ike at 12 NDBC buoys. The measured data is shown with black dots, and the modeled SWAN results are shown with black lines.

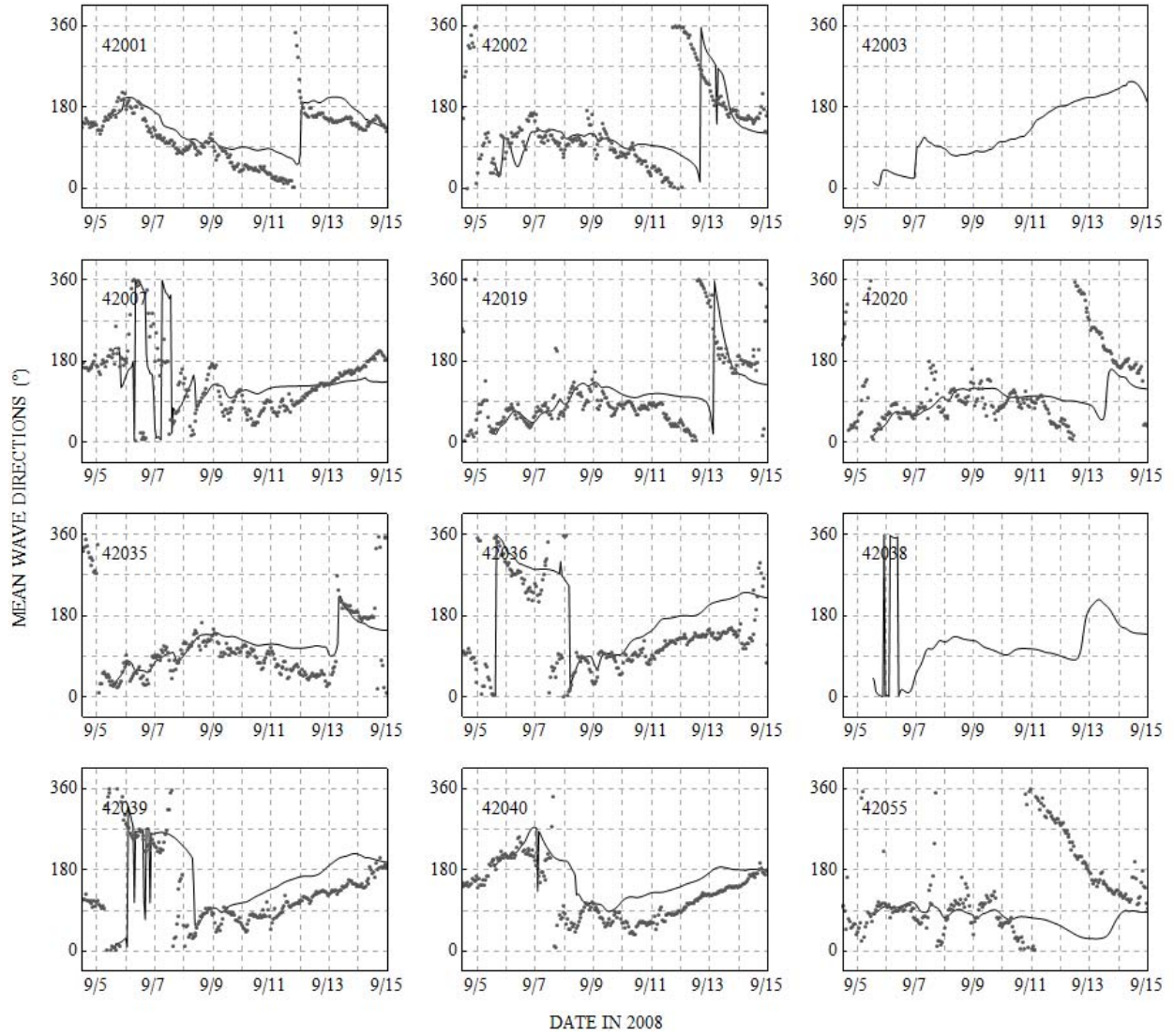


Figure 11: Mean wave directions (°), measured clockwise from geographic north, during Hurricane Ike at 12 NDBC buoys. The measured data is shown with black dots, and the modeled SWAN results are shown with black lines.

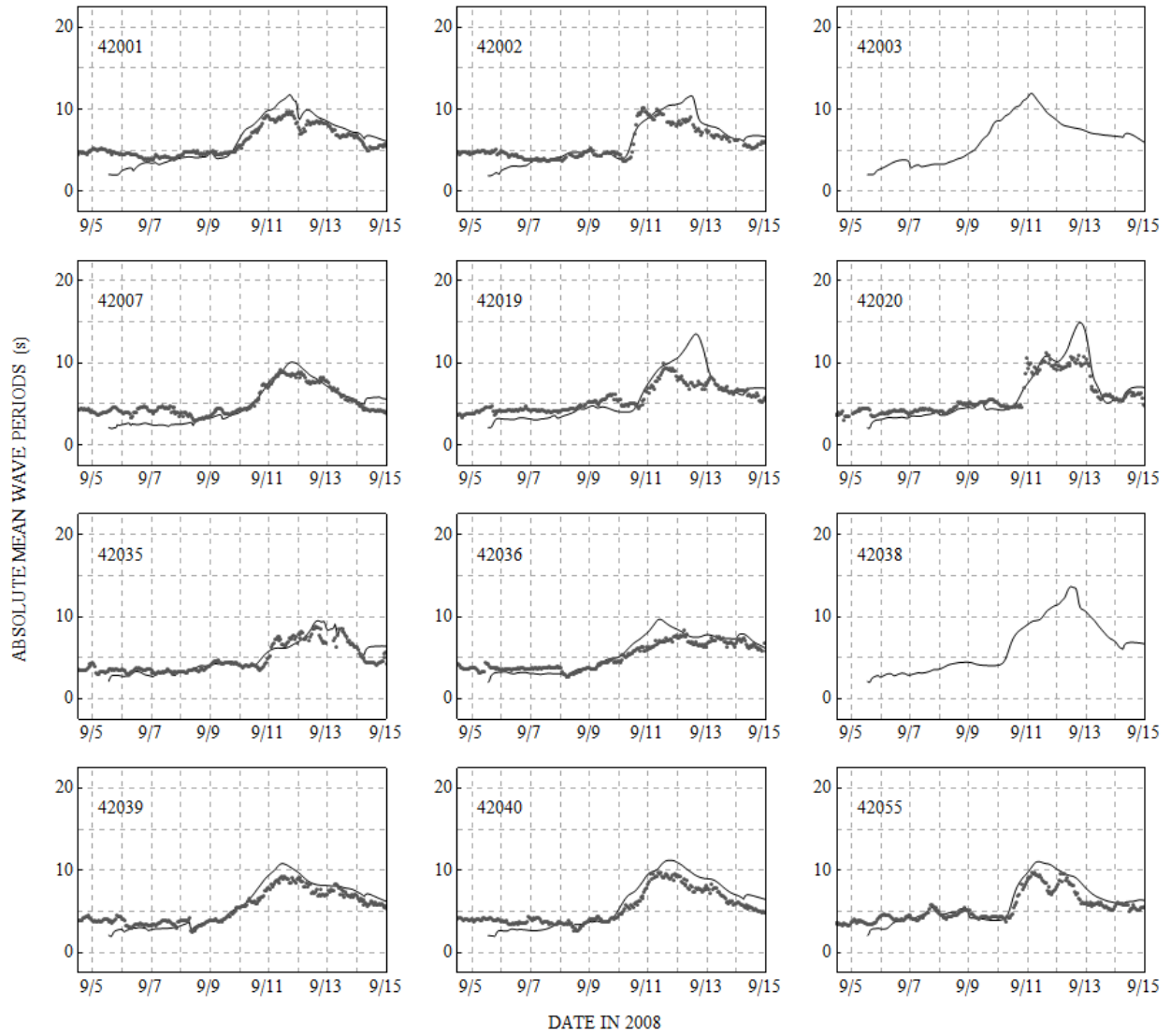


Figure 12: Mean wave periods (s) during Hurricane Ike at 12 NDBC buoys. The measured data is shown with black dots, and the modeled SWAN results are shown with black lines.

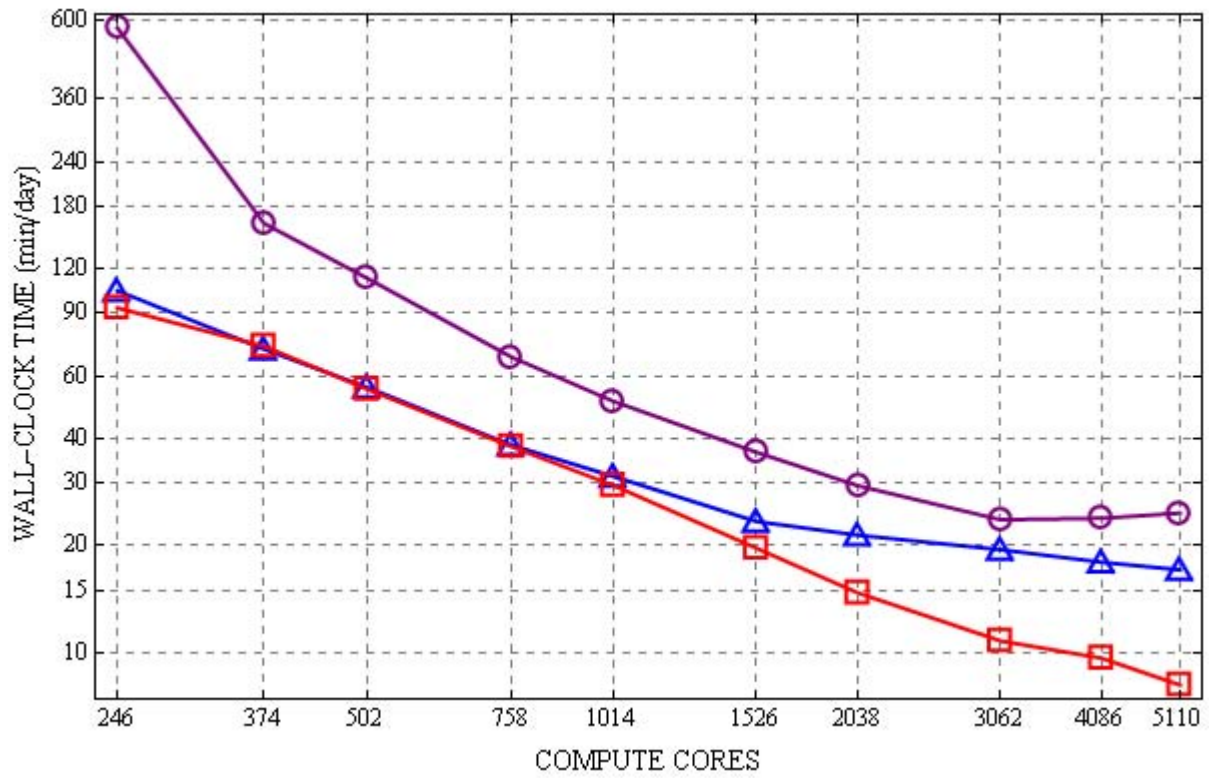


Figure 13: Timing results for SWAN+ADCIRC and its components on the TACC Ranger machine. The times shown are wall-clock minutes per day of Katrina simulation on the SL15 grid. SWAN results are shown in red, ADCIRC results are shown in blue, and SWAN+ADCIRC results are shown in purple.

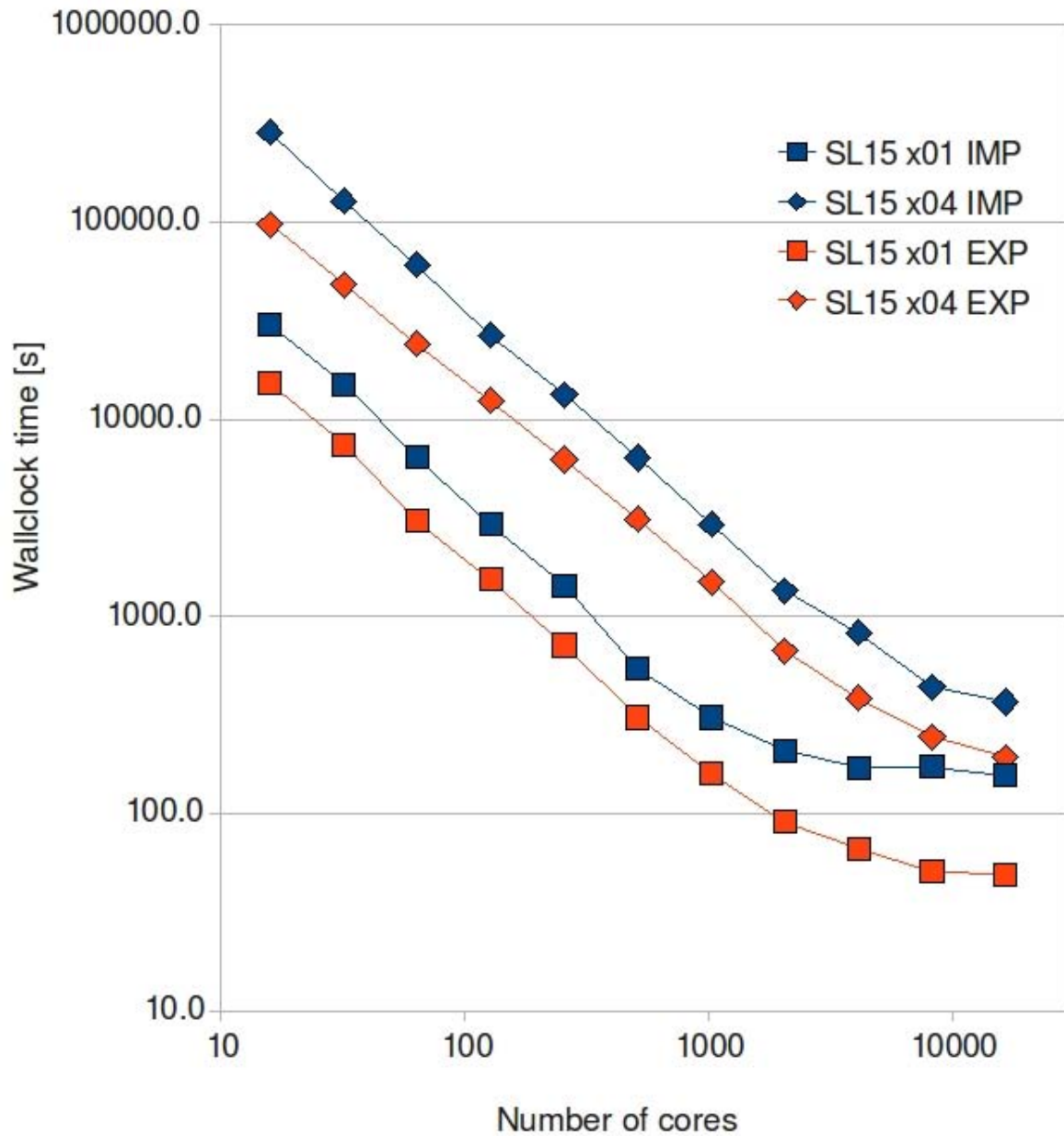


Figure 14: Performance as a function of the number of cores of the SL15 grid implicit (with 1 sec time step), SL15x04 grid implicit (with 0.5 sec time step), SL15 grid explicit (with 1 second time step), and SL15x04 grid explicit (with 0.5 second time step) ADCIRC-CG simulations on Ranger. Wall clock time is in seconds for a 0.25 days tidal simulation.

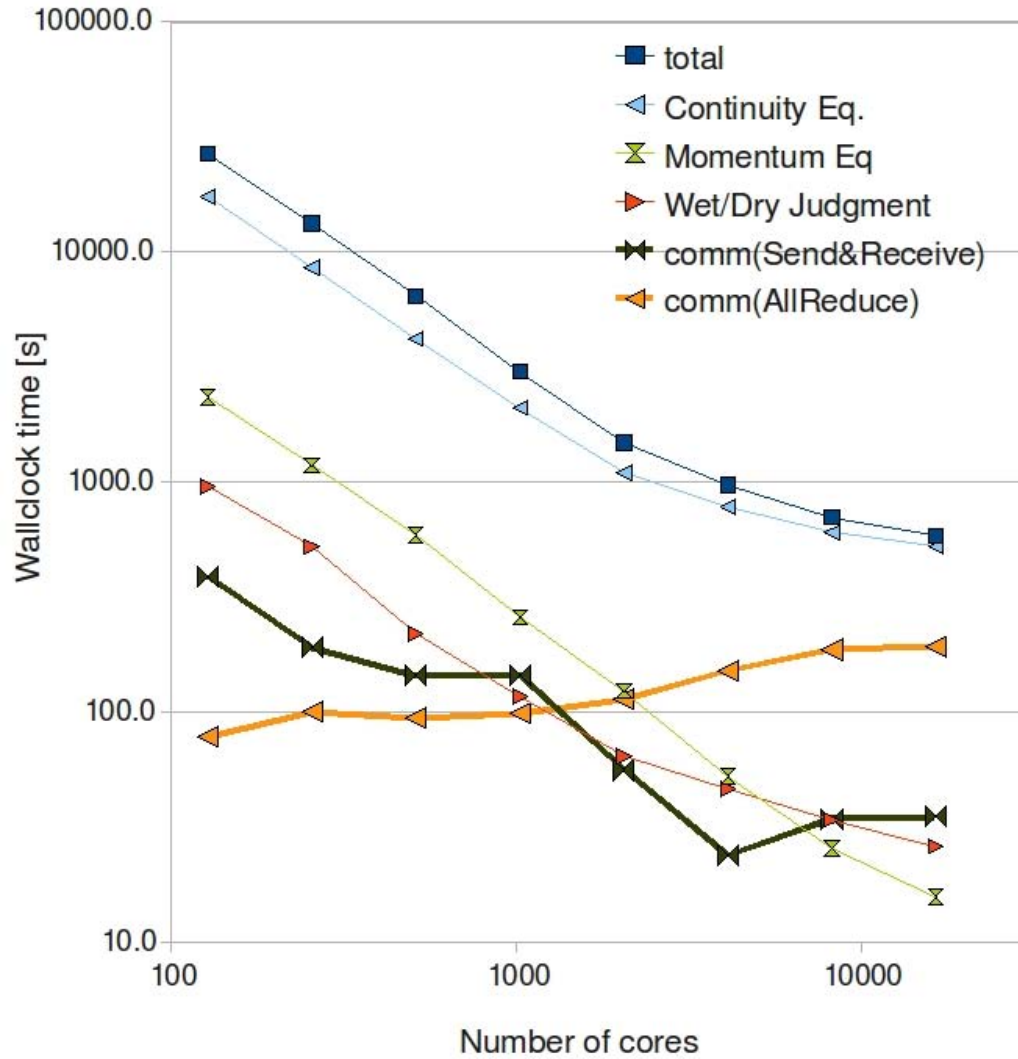


Figure 15: Component performance of the SL15-04x grid with implicit ADCIRC-CG simulation on Ranger. Wall clock times are in seconds per one day of simulation time and normalized to 1 second time steps. Components examined include total time; the continuity (GWCE) equation; momentum equation; wet/dry evaluation; local communication between overlapping layers of adjacent subdomains; global communication used the MPI all reduce associated with the implicit code matrix solution.

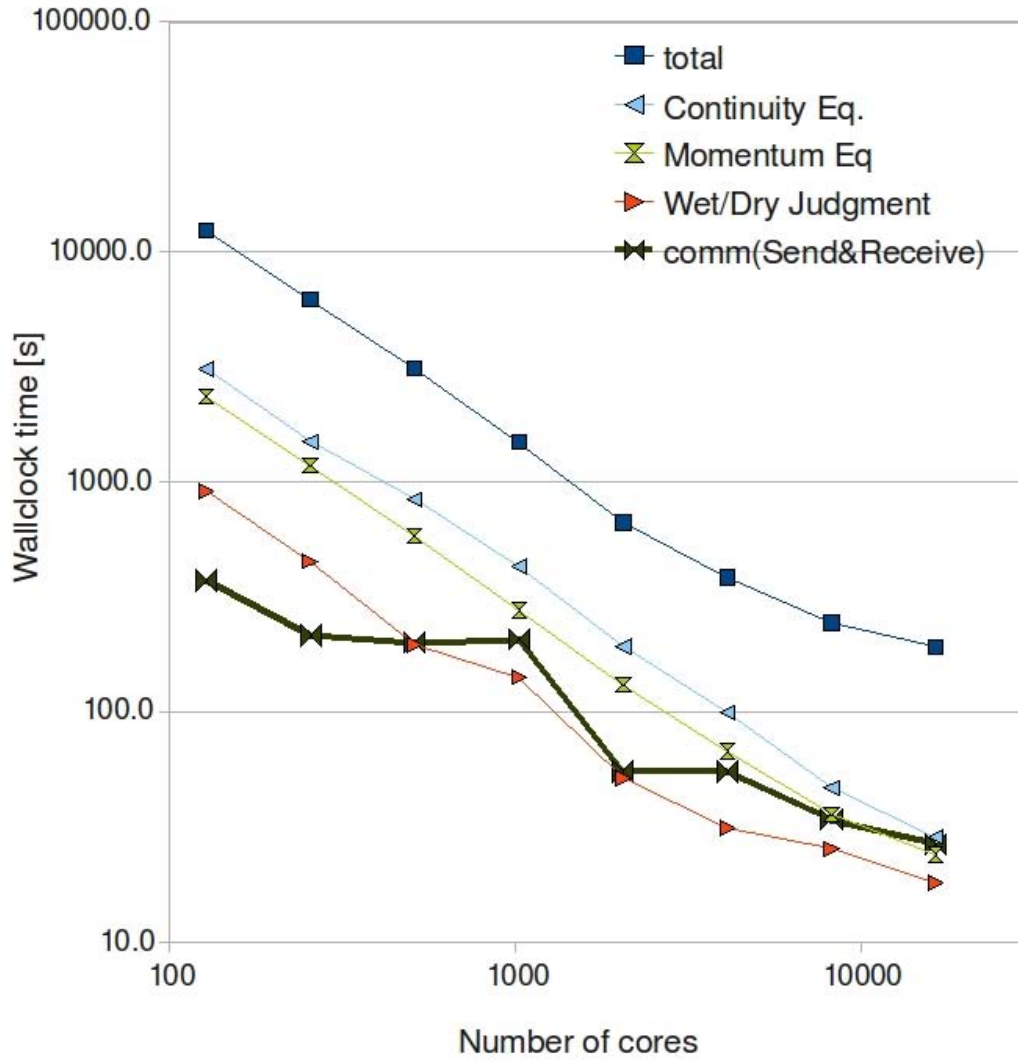


Figure 16: Component performance of the SL15-04x grid with explicit ADCIRC-CG simulation on Ranger. Wall clock times are in seconds per one day of simulation time and are normalized to one second time steps. Components examined include total time; the continuity (GWCE) equation; momentum equation; wet/dry evaluation; local communication between overlapping layers of adjacent subdomains.

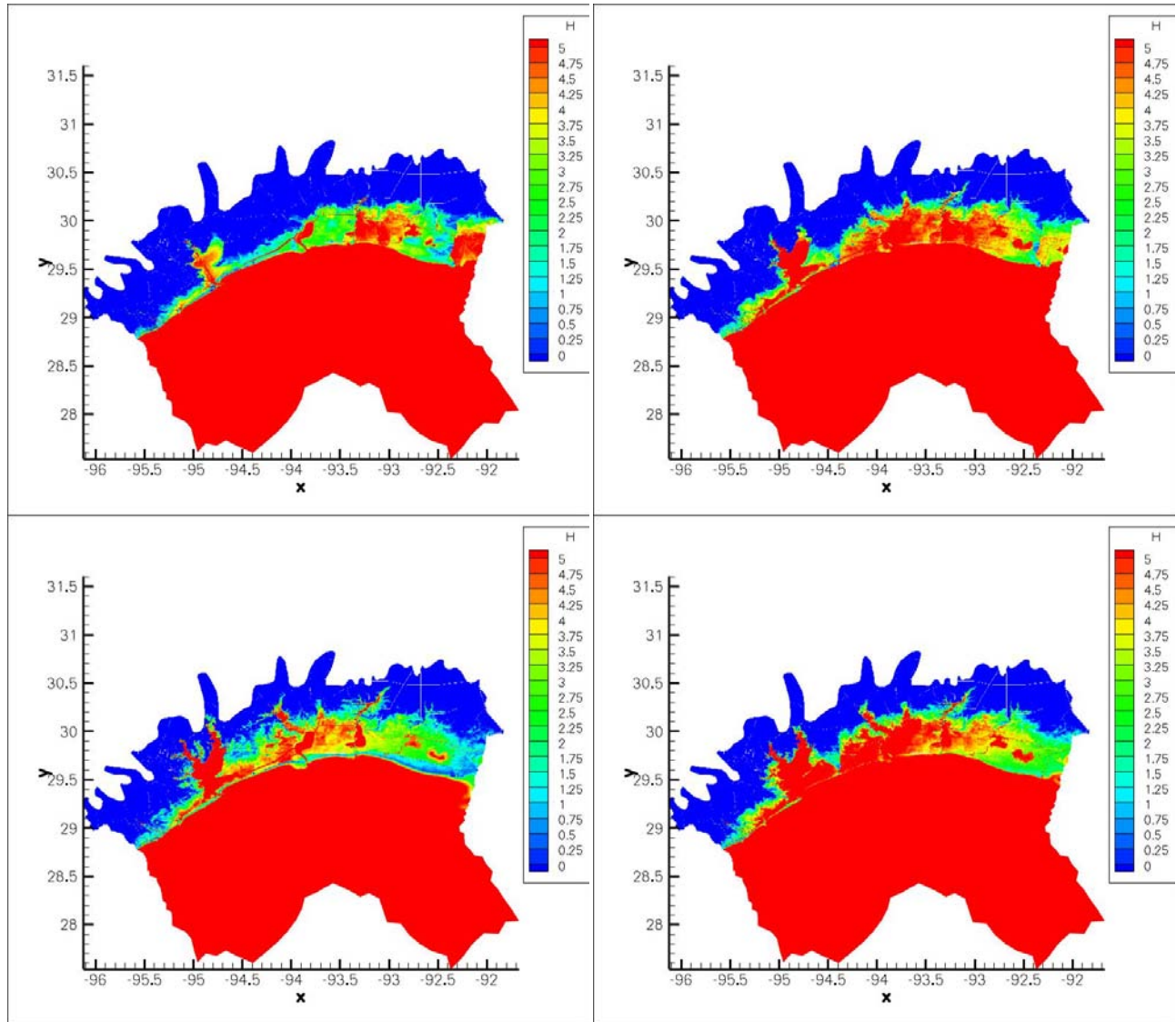


Figure 17: ADCIRC DG computed water column height (m) during Hurricane Ike along the Texas coastline.

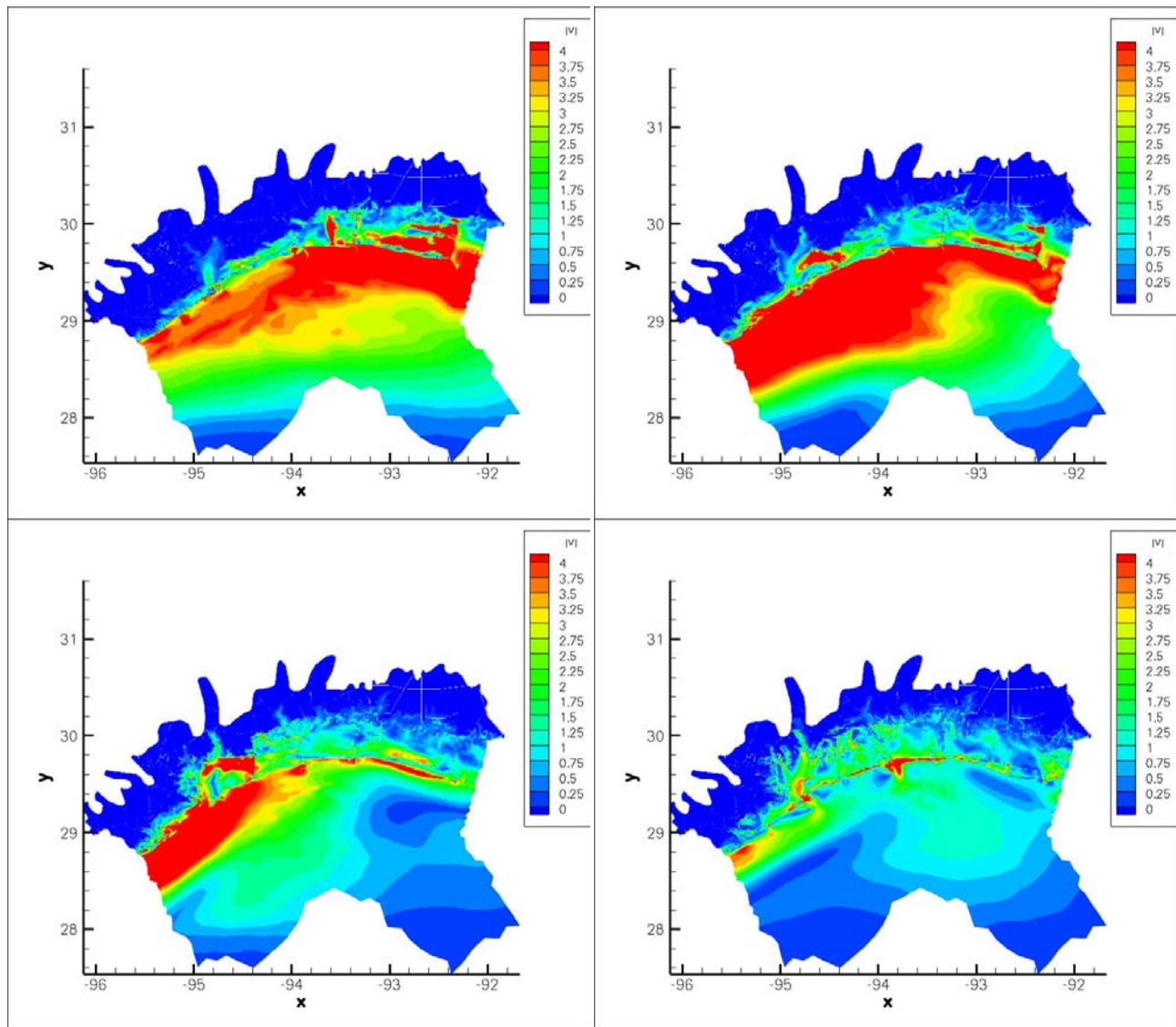


Figure 18: ADCIRC DG computed velocity (m/s) during Hurricane Ike along the Texas coastline.